Anomalous scaling of fermions and order parameter fluctuations at quantum criticality

P. Strack,[*] S. Takei, and W. Metzner

Max-Planck-Institute for Solid State Research, Heisenbergstrasse 1, D-70569 Stuttgart, Germany
(Received 24 May 2009; revised manuscript received 22 November 2009; published 4 March 2010)

We analyze the quantum phase transition between a semimetal and a superfluid in a model of attractively interacting fermions with a linear dispersion. The quantum critical properties of this model cannot be treated by the Hertz-Millis approach since integrating out the fermions leads to a singular Landau-Ginzburg order parameter functional. We therefore derive and solve coupled renormalization-group equations for the fermionic degrees of freedom and the bosonic order parameter fluctuations. In two spatial dimensions, fermions and bosons acquire anomalous scaling dimensions at the quantum critical point, associated with non-Fermi-liquid behavior and non-Gaussian order parameter fluctuations.

I. INTRODUCTION

As noticed already more than 30 years ago by Hertz,[1] quantum phase transitions in correlated fermion systems may be described in terms of the order parameter field alone when one integrates out fermions from the path integral in one stroke and subsequently deals with an exclusively bosonic theory. The resultant effective action is expanded in powers of the bosonic field ϕ and often truncated after the ϕ^4 term. Although an analysis in terms of ϕ^4-type theories seems mundane, the presence of *two* relevant energy scales, one given by temperature and the other given by a nonthermal control parameter acting as a mass term in the bosonic propagator, gives rise to a rich finite temperature phase diagram.[2]

The Hertz-Millis approach relies on integrating out fermions first. In general, however, the fermions are gapless and consequently may lead to singular coefficients in the effective bosonic action.[3,4] In such cases, it is advisable to keep the fermions in the theory and treat them on equal footing with the bosons. Various coupled Fermi-Bose systems exhibiting quantum criticality have been analyzed previously.[5–11] The complicated interplay of two singular propagators promotes a controlled treatment to a formidable task.

A suitable tool to cope with the interplay of fermionic and bosonic fluctuations is the functional renormalization group (RG) formulated for fermionic and bosonic fields.[12–15] The mutual feedback of gapless fermions coupled to massless bosons has been studied already with functional flow equations for quantum electrodynamics (QED),[16] non-Abelian gauge theories,[17] and the Gross-Neveu model.[18]

The purpose of the present paper is to show how one can—within the coupled Fermi-Bose RG framework—obtain non-Fermi-liquid properties of quantum critical fermion systems for which the Hertz-Millis approach is not applicable. To this end, we study a "Dirac cone" model of attractively interacting fermions with a linear dispersion, which exhibits a quantum phase transition from a semimetal to a superfluid at a finite interaction strength as shown in Fig. 1. The coupled fermion-boson flow equations are physically transparent and a relatively simple truncation seems to capture the essential renormalizations. As a central result, the fermion and order parameter propagators develop anomalous power-law dependences on frequency and momentum at the quantum critical point (QCP) in dimensions $d < 3$.

In Sec. II, we introduce the attractive Dirac cone model and the associated Fermi-Bose action. Subsequently, in Sec.

III, we show that a mean-field treatment of this model leads to a semimetal-to-superfluid quantum phase transition at a critical interaction strength U_c. In Sec. IV, the RG method, truncation and flow equations are presented. Results for the quantum critical behavior follow in Sec. V. We finally summarize and conclude in Sec. VI.

II. DIRAC CONE MODEL

We consider an interacting fermion system with the bare action

$$\Gamma_0[\psi, \bar{\psi}] = -\int_{k\alpha\sigma} \bar{\psi}_{k\alpha\sigma}(ik_0 - \xi_{\mathbf{k}\alpha})\psi_{k\alpha\sigma}$$
$$+ U\int_{k\alpha}\int_{k'\alpha'}\int_q \bar{\psi}_{-k,\alpha\downarrow}\bar{\psi}_{k+q,\alpha\uparrow}\psi_{k'+q,\alpha'\uparrow}\psi_{-k',\alpha'\downarrow}.$$
$$(1)$$

The variables $k = (k_0, \mathbf{k})$ and $q = (q_0, \mathbf{q})$ collect Matsubara energies and momenta, and we use the shorthand notation $\int_k = \int_{-\infty}^{\infty} \frac{dk_0}{2\pi}\int\frac{d^d\mathbf{k}}{(2\pi)^d}$ for momentum and energy integrals; $\int_{k\alpha}$ includes also the sum over the band index $\alpha = \pm 1$ and $\int_{k\alpha\sigma}$ includes also the spin sum over $\sigma = \uparrow, \downarrow$. Our analysis is restricted to zero temperature such that the Matsubara energies are continuous variables. The dispersion of the fermions is given by the Dirac cone

$$\xi_{\mathbf{k}\alpha} = \alpha v_f |\mathbf{k}|,\quad\quad\quad (2)$$

corresponding to massless particles with positive ($\alpha = 1$) and negative ($\alpha = -1$) energy. The chemical potential is chosen as
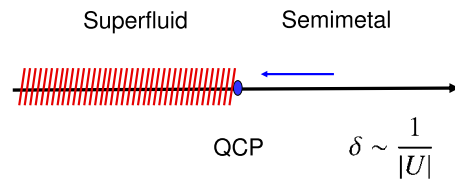

FIG. 1. (Color online) Schematic phase diagram of the attractive Dirac cone model at zero temperature. The QCP at a critical interaction strength U_c separates the semimetal from the superfluid. In this paper, we approach the QCP from the semimetallic phase as indicated by the arrow.
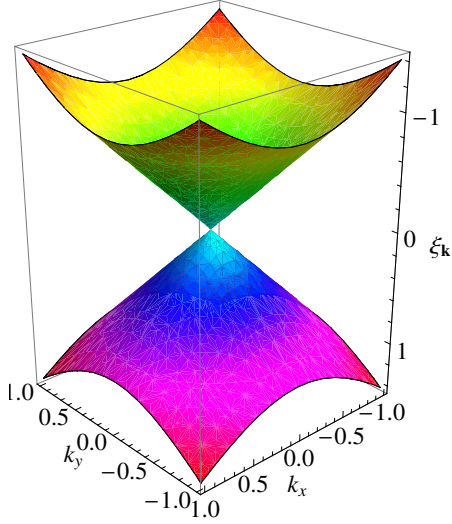
FIG. 2. (Color online) Dirac cone dispersion in two dimensions.

$\mu=0$, such that in the absence of interactions states with negative energy are filled, while states with positive energy are empty. The Fermi surface thus consists only of one point, the "Dirac point" at $\mathbf{k}=\mathbf{0}$, where the two cones in Fig. 2 intersect. Momentum integrations are cutoff in the ultraviolet by the condition $|\xi_{\mathbf{k}\alpha}|<\Lambda_0$. The kinetic energy in Eq. (1) is a simplified version of the dispersion for electrons moving on a honeycomb lattice as in graphene, where the momentum dependence is entangled with a pseudospin degree of freedom related to the two-atom structure of the unit cell.[19]

The two-particle interaction in Eq. (1) is parameterized by a momentum-independent coupling constant U and corresponds to a local interaction in real space. Note that the kinetic energy and the interaction are both diagonal in the spin indices. Although our model is reminiscent of the Gross-Neveu model,[20] it is not equivalent to it. In particular, for the Gross-Neveu model there is no choice of a spinor basis in which the kinetic and potential energies are both spin diagonal. The Gross-Neveu model is Lorentz invariant while our model is not.

For attractive interactions, the coupling constant U is negative and drives spin singlet pairing associated with spontaneous breaking of the global $U(1)$ gauge symmetry. Therefore, we decouple the interaction in the s-wave spin-singlet pairing channel by introducing a complex bosonic Hubbard-Stratonovich field ϕ conjugate to the bilinear composite of fermionic fields $U\int_{k\alpha}\psi_{k+q,\alpha\uparrow}\psi_{-k,\alpha\downarrow}$.[21] This yields a functional integral over ψ, $\bar{\psi}$, and ϕ with the new bare action

$$
\Gamma_0[\psi,\bar{\psi},\phi]=-\int_{k\alpha\sigma}\bar{\psi}_{k\alpha\sigma}(ik_0-\xi_{\mathbf{k}\alpha})\psi_{k\alpha\sigma}-\int_q\phi_q^*\frac{1}{U}\phi_q
$$
$$
+\int_{k\alpha}\int_q(\bar{\psi}_{-k,\alpha\downarrow}\bar{\psi}_{k+q,\alpha\uparrow}\phi_q+\psi_{k+q,\alpha\uparrow}\psi_{-k,\alpha\downarrow}\phi_q^*),
$$
$$
(3)
$$

where ϕ^* is the complex conjugate of ϕ while ψ and $\bar{\psi}$ are

algebraically independent Grassmann variables. The boson mass $\delta=-1/U$ plays the role of the control parameter for the quantum phase transition.

III. MEAN-FIELD THEORY

Neglecting bosonic fluctuations by replacing ϕ_q with its expectation value $\phi_{q=0}$, the saddle-point approximation solves the functional integral of Eq. (3) and leads to the standard BCS gap equation[21]

$$
\phi_0=-U\int_{k\alpha}\frac{\phi_0}{k_0^2+\xi_{\mathbf{k}\alpha}^2+\phi_0^2}.
\qquad (4)
$$

The critical interaction strength U_c, beyond which the gap equation has a solution with nonzero ϕ_0, is given by

$$
\frac{1}{U_c}=-\int\frac{dk_0}{2\pi}\int_{-\Lambda_0}^{\Lambda_0}d\xi N(\xi)\frac{1}{k_0^2+\xi^2},
\qquad (5)
$$

where the density of states has the form

$$
N(\xi)=\frac{K_d}{v_f^d}|\xi|^{d-1}
\qquad (6)
$$

with K_d being defined by $\int\frac{d^dk}{(2\pi)^d}=K_d\int d|\mathbf{k}||\mathbf{k}|^{d-1}$. Since the density of states vanishes at the Fermi level (for $d>1$), the system is stable against pairing for a weak attraction. Instead, a finite attraction beyond a certain threshold is necessary to cause superfluidity even at zero temperature. Performing the integrations in Eq. (5), we obtain the mean-field position of the quantum phase transition in Fig. 1. In two dimensions, we have

$$
\delta_c^{\mathrm{MFT}}=-\frac{1}{U_c^{\mathrm{MFT}}}=\frac{\Lambda_0}{2\pi v_f^2}.
\qquad (7)
$$

Upon setting $v_f=\Lambda_0=1$, the numerical value for the mean-field control parameter value is $\delta_c^{\mathrm{MFT}}=0.159$.

A similar quantum phase transition from a semimetal to a superfluid has been discussed previously for attractively interacting electrons on a honeycomb lattice in the context of ultracold atoms[22] and graphene.[23] In the following, we take fluctuations into account by performing a renormalization-group analysis which enables us to compute the quantum critical exponents at and in the vicinity of the QCP.

IV. RG METHOD

We derive flow equations for the scale-dependent effective action $\Gamma^\Lambda[\psi,\bar{\psi},\phi]$ within the functional RG framework for fermionic and bosonic degrees of freedom in its one-particle irreducible representation.[12–15] Starting from the bare fermion-boson action $\Gamma^{\Lambda=\Lambda_0}[\psi,\bar{\psi},\phi]=\Gamma_0[\psi,\bar{\psi},\phi]$ in Eq. (3), fermionic and bosonic fluctuations are integrated *simultaneously*, proceeding from higher to lower scales as parameterized by the continuous flow parameter Λ. In the infrared limit $\Lambda\to0$, the fully renormalized effective action $\Gamma^{\Lambda\to0}[\psi,\bar{\psi},\phi]$ is obtained.

The flow of Γ^Λ is governed by the exact functional flow equation[12–15]

$$\frac{d}{d\Lambda}\Gamma^\Lambda[\psi,\bar\psi,\phi] = \mathrm{Str}\frac{\partial_\Lambda R^\Lambda}{\Gamma^{(2)\Lambda}[\psi,\bar\psi,\phi]+R^\Lambda}, \tag{8}$$

where $\Gamma^{(2)\Lambda}$ denotes the second functional derivative with respect to the fields and R^Λ is the infrared regulator (to be specified below). The supertrace (Str) traces over all indices with an additional minus sign for fermionic contractions. When evolving Γ^Λ, infinitely many terms involving fermionic and/or bosonic fields with possibly complicated dependences on frequencies and momenta are generated, necessitating a truncation of the effective action.

A. Truncation

We now explain how the effective action is truncated with the objective to capture the essential renormalization effects.

1. Fermion propagator

To account for the renormalization of the fermionic single-particle properties by order parameter fluctuations, the quadratic fermionic term in the action is multiplied by a field renormalization factor Z_f,

$$\Gamma_{\bar\psi\psi} = -\int_{k\alpha\sigma} \bar\psi_{k\alpha\sigma} Z_f (ik_0 - \xi_{\mathbf{k}\alpha}) \psi_{k\alpha\sigma}, \tag{9}$$

yielding the fermion propagator

$$G_{f\alpha}(k) = -\langle\psi_{k\alpha\sigma}\bar\psi_{k\alpha\sigma}\rangle = \frac{Z_f^{-1}}{ik_0 - \xi_{\mathbf{k}\alpha}}. \tag{10}$$

A diverging Z_f suppresses the quasiparticle weight to zero, leading to non-Fermi-liquid behavior. The Fermi velocity is not renormalized separately but kept fixed, since for the linear-dispersion relation, Eq. (2), the renormalization of the term proportional to k_0 and the one proportional to $\xi_{\mathbf{k}\alpha}$ in $\Gamma_{\bar\psi\psi}$ differ only by a finite factor of order 1. The initial condition for Z_f is $Z_f = 1$.

2. Boson propagator

The bosonic quadratic part of the bare action, Eq. (3), consists only of a local mass term. Integrating out fluctuations, a momentum and frequency dependence is generated, in particular, by fermionic contributions involving the fermionic particle-particle bubble. For small momenta and frequencies this dependence is quadratic, leading to the following ansatz for the bosonic quadratic part of the action

$$\Gamma_{\phi^*\phi} = \int_q \phi_q^*[Z_b(q_0^2+\mathbf{q}^2)+\delta]\phi_q. \tag{11}$$

Note that there is no linear term in frequency here, as we consider the half-filled band and the usual (imaginary) linear frequency part of the particle-particle bubble vanishes exactly due to particle-hole symmetry. The parameter δ controls the distance to the quantum phase transition and is also renormalized by fluctuations. If the initial value of δ is tuned
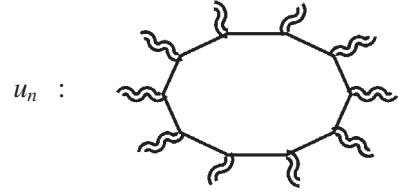

FIG. 3. Fermion loop which generates the bosonic $2n$-point vertex, here for $n=5$.

so that $\delta\to 0$ for vanishing cutoff $\Lambda\to 0$, we are at the quantum critical point. The boson propagator, parameterized by two flowing parameters, Z_b and δ, reads

$$G_b(q) = -\langle\phi_q\phi_q^*\rangle = -\frac{1}{Z_b(q_0^2+\mathbf{q}^2)+\delta}. \tag{12}$$

The initial condition for the control parameter is $\delta=-1/U$. The initial condition for Z_b corresponding to the bare action in Eq. (3) is $Z_b=0$. However, starting the flow with $Z_b=0$ leads to very large transient anomalous dimensions at the initial stage of the flow (for Λ near Λ_0), which complicates the analysis in a (high-energy) regime which is physically not interesting. The low-energy flow (small $\Lambda\to 0$) does not depend on the initial value of Z_b. We therefore add a term $\int\phi_q^*(q_0^2+\mathbf{q}^2)\phi_q$ to the bare action corresponding to an initial value $Z_b=1$. This term regularizes our model by suppressing the interaction for large momentum and energy transfers.

3. Order parameter self-interaction

In the Hertz-Millis theory of quantum criticality[1,2] one expands the order parameter self-interaction in (even) powers of the bosonic fields,

$$\Gamma_I[\phi] = \sum_{n\geq 2} u_{2n}\int (\phi^*\phi)^n, \tag{13}$$

where the coefficients u_{2n} are generated by fermion loops with $2n$ fermion propagators and $2n$ external bosonic legs as shown in Fig. 3. At finite temperatures or when the fermions are gapped, the integrals corresponding to these loops are finite. With the bare, gapless fermion propagator at zero temperature, however, the loops diverge for vanishing external momenta

$$u_{2n} \sim \int d^{d+1}k \frac{1}{(k_0^2+\xi_{\mathbf{k}}^2)^n} \sim \frac{1}{\Lambda^{2n-(d+1)}}, \tag{14}$$

where Λ is an infrared cutoff introduced here merely to specify the degree of the divergence. In particular, the ϕ^4 interaction diverges as $u_4\sim 1/\Lambda$ in two dimensions. For the present case of fermionic loops with pairing vertices, there are no cancellations which reduce the divergence below the level of simple power counting. This is in stark contrast to the situation for instabilities driven by forward scattering, where oscillating integrands and cancellations between permutations of external legs render the loops finite in the low-energy limit.[24,25]

The divergence of the fermion loops makes the Hertz-Millis approach of expanding the effective action in powers

of the ordering field alone inapplicable. Besides issues related to the increasing degree of divergence of higher-order interactions, already at the quartic level one would face the problem to parameterize the complicated singular momentum dependence of the interaction generated by the fermionic loop. Integrating the fermions along with the bosons in a coupled RG flow, the vertices remain finite and can be parameterized by a momentum-independent running coupling as usual. In particular, the ϕ^4 term, which is generated by fermionic fluctuations, but then also influenced by bosonic fluctuations, can be written as

$$\Gamma_{|\phi|^4} = \frac{u}{8} \int_{q,q',p} \phi_{q+p}^* \phi_{q'-p}^* \phi_{q'} \phi_q. \tag{15}$$

The initial condition for u is $u = 0$.

4. Fermion-boson vertex

The fermion-boson vertex has the form

$$\Gamma_{\psi^2 \phi^*} = g \int_{k\alpha} \int_q (\bar{\psi}_{-k,\alpha\downarrow} \bar{\psi}_{k+q,\alpha\uparrow} \phi_q + \psi_{k+q,\alpha\uparrow} \psi_{-k,\alpha\downarrow} \phi_q^*). \tag{16}$$

The fermion-boson vertex is not renormalized within our truncation. The usual one-loop vertex correction, which is formally of order g^3, vanishes in the normal phase due to particle conservation.[15] Hence, the coupling g remains invariant at its bare value $g = 1$ in the course of the flow. By contrast, the fermion-boson vertex obtained by decoupling the interaction of the Gross-Neveu model[20] via a Hubbard-Stratonovich field is renormalized already at one-loop level.

Symmetry breaking in interacting Fermi systems is frequently studied by extending the model to an arbitrary number of fermion flavors N_f and expanding in the parameter $1/N_f$. Our truncation captures the leading contributions for large N_f. Below we will see that the low-energy behavior is captured correctly also to leading order in ϵ, where $\epsilon = 3 - d$ is the deviation from the critical spatial dimension $d_c = 3$, below which anomalous scaling sets in.

B. Flow equations

In Sec. IV B, we derive the flow equations for our truncated effective action. Both propagators, Eqs. (10) and (12), display singularities for vanishing momenta and frequencies, the zero-temperature fermion propagator everywhere in the semimetallic phase, and the boson propagator at the QCP when the bosonic mass vanishes. These infrared singularities are regularized by adding optimized momentum cutoffs[26] for fermions (subscript f) and bosons (subscript b),

$$R_{f\alpha}^\Lambda(\mathbf{k}) = Z_f(\Lambda \, \mathrm{sgn}[\xi_{\mathbf{k}\alpha}] - \xi_{\mathbf{k}\alpha}) \theta[\Lambda - |\xi_{\mathbf{k}\alpha}|],$$

$$R_b^\Lambda(\mathbf{q}) = Z_b(\Lambda^2 - \mathbf{q}^2) \theta[\Lambda^2 - \mathbf{q}^2], \tag{17}$$

to the inverse of the propagators. We denote the regularized propagators by $G_{f\alpha}^R$ and G_b^R. Note that we have set $v_f = 1$, such that Λ is a common momentum cutoff for fermions and bosons, which is a frequent choice for critical fermion-boson
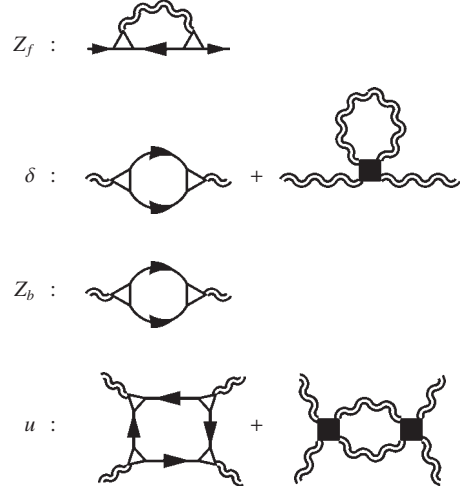

FIG. 4. Feynman diagrams representing the flow equations.

theories.[16,26] The scale derivatives of the cutoffs read,

$$\partial_\Lambda R_{f\alpha}^\Lambda(\mathbf{k}) = Z_f \, \mathrm{sgn}[\xi_{\mathbf{k}\alpha}] \theta[\Lambda - |\xi_{\mathbf{k}\alpha}|],$$

$$\partial_\Lambda R_b^\Lambda(\mathbf{q}) = 2Z_b \Lambda \, \theta[\Lambda^2 - \mathbf{q}^2], \tag{18}$$

where terms proportional to $\partial_\Lambda Z_f$ and $\partial_\Lambda Z_b$ are neglected. These additional terms are of higher order in the vertices. Arguments buttressing this commonly employed approximation are given in Ref. 12.

The recipe to obtain the flow equations is now the following: one executes a cutoff derivative acting on $R_{f,b}^\Lambda$ in the analytic expressions corresponding to all one-loop one-particle irreducible Feynman diagrams for the parameters Z_f, Z_b, δ, u, which can be constructed with the interaction vertices and the regularized propagators $G_{f\alpha}^R$ and G_b^R, as shown in Fig. 4. For the cutoff derivative and loop integration we use the shorthand notation

$$\int_k^R = \int \frac{dk_0}{2\pi} \int \frac{d^d k}{(2\pi)^d} \sum_{s=b,f} (-\dot{R}_s^\Lambda) \partial_{R_s^\Lambda}. \tag{19}$$

The feedback of bosonic fluctuations on the fermionic propagator is captured by the self-energy diagram in the first line of Fig. 4, leading to the flow equation for the fermionic Z factor

$$\partial_\Lambda Z_f = g^2 \int_q^R \frac{\partial}{i \, \partial k_0} G_{f\alpha}^R(q-k) G_b^R(q) \Big|_{k=0}. \tag{20}$$

Note that there is no sum over α here and $\alpha = \pm 1$ yields the same Z_f.

For the control parameter, we evaluate the diagrams with two external bosonic legs, obtaining the two contributions

$$\partial_\Lambda \delta = g^2 \int_{k\alpha}^R G_{f\alpha}^R(k) G_{f\alpha}^R(-k) + \frac{u}{2} \int_q^R G_b^R(q). \tag{21}$$

The fermionic contribution on the right-hand side is positive leading to a reduction in δ for decreasing Λ, whereas the bosonic contribution tends to increase δ.

The flow of the bosonic Z factor is obtained as the second frequency derivative of the fermionic particle-particle bubble,

$$\partial_\Lambda Z_b = g^2 \int_{k\alpha}^R \frac{1}{2} \frac{\partial^2}{\partial q_0^2} G_{f\alpha}^R(k+q) G_{f\alpha}^R(-k) \bigg|_{q=0}. \quad (22)$$

The bosonic tadpole diagram does not contribute here, as the ϕ^4 vertex u is taken as momentum and frequency independent.

Finally, the bosonic self-interaction flows according to

$$\partial_\Lambda u = -4g^4 \int_{k\alpha}^R [G_{f\alpha}^R(-k)]^2 [G_{f\alpha}^R(k)]^2 + \frac{5}{4} u^2 \int_q^R [G_b^R(q)]^2, \quad (23)$$

where the first terms generates u and the second, bosonic term tends to reduce u in the course of the flow.

All frequency and momentum integrations in the above flow equations can be performed analytically. We now eliminate explicit Λ dependences from the flow equations by employing the following scaling variables

$$\tilde{\delta} = \frac{\delta}{\Lambda^2 Z_b},$$

$$\tilde{g} = \frac{g\sqrt{K_d}}{\Lambda^{(3-d)/2} Z_f \sqrt{Z_b} \sqrt{d}},$$

$$\tilde{u} = \frac{u K_d}{\Lambda^{3-d} Z_b^2 d}. \quad (24)$$

Dependences on the Z factors are absorbed by introducing the anomalous dimensions for fermionic and bosonic fields,

$$\eta_f = -\frac{d \log Z_f}{d \log \Lambda},$$

$$\eta_b = -\frac{d \log Z_b}{d \log \Lambda}. \quad (25)$$

The flow equations for the control parameter and the bosonic self-interaction are then obtained as

$$\frac{d\tilde{\delta}}{d \log \Lambda} = (\eta_b - 2)\tilde{\delta} + \tilde{g}^2 - \frac{\tilde{u}}{4(1+\tilde{\delta})^{3/2}},$$

$$\frac{d\tilde{u}}{d \log \Lambda} = (d - 3 + 2\eta_b)\tilde{u} - 6\tilde{g}^4 + \frac{15}{16}\frac{\tilde{u}^2}{(1+\tilde{\delta})^{5/2}}. \quad (26)$$

The rescaled fermion-boson vertex $\tilde{g}$ obeys the equation

$$\frac{d\tilde{g}}{d \log \Lambda} = \left(\eta_f + \frac{1}{2}\eta_b - \frac{3-d}{2}\right)\tilde{g}. \quad (27)$$

The Eqs. (26) and (27) have to be considered in conjunction with the boson and fermion anomalous dimensions
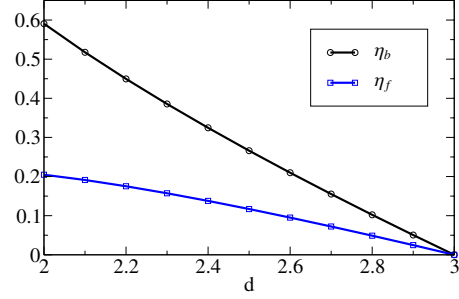
$$\eta_b = \frac{3}{4}\tilde{g}^2,$$

FIG. 5. (Color online) Fermion and boson anomalous exponents at the QCP for $2 \leq d \leq 3$.

$$\eta_f = \frac{\tilde{g}^2}{2}\left[\frac{1}{(1+\tilde{\delta})^{3/2}} + \frac{2}{(1+\tilde{\delta})}\right]\frac{1}{2+\tilde{\delta}+2\sqrt{1+\tilde{\delta}}}. \quad (28)$$

We recall that we have set the Fermi velocity $v_f = 1$. We will now investigate the fixed point of these equations and then solve them numerically.

V. SOLUTION AT THE QUANTUM CRITICAL POINT

A. Fixed point

At the quantum critical point, the system is scale invariant at low energies. The scaling regime is associated with a fixed point of the flow equations, which attracts the flow for small Λ. The fixed point is defined by the condition that the right-hand sides of the flow equations for $\tilde{\delta}$, $\tilde{u}$, and $\tilde{g}$ vanish, such that

$$\frac{d\tilde{\delta}}{d \log \Lambda} = \frac{d\tilde{g}}{d \log \Lambda} = \frac{d\tilde{u}}{d \log \Lambda} = 0. \quad (29)$$

One thus has to solve three algebraic equations together with the equations for the anomalous exponents, Eq. (28). The fermion-boson vertex $\tilde{g}$ and the boson self-interaction $\tilde{u}$ are relevant couplings below three dimensions, and the flow equations for $\tilde{g}$ and $\tilde{u}$ have stable non-Gaussian ($\tilde{g} \neq 0$, $\tilde{u} \neq 0$) solutions with finite anomalous exponents η_f and η_b. The condition $\frac{d\tilde{g}}{d \log \Lambda} = 0$ directly implies a relation between the anomalous dimensions

$$\eta_f + \frac{\eta_b}{2} = \frac{3-d}{2}. \quad (30)$$

The values of η_f and η_b as obtained from a numerical solution of the fixed-point equations are plotted in Fig. 5 as a function of dimensionality d for $2 \leq d \leq 3$.

The anomalous dimensions vanish at the critical dimension $d_c = 3$. It is instructive to solve the fixed-point equations analytically to leading order in $\epsilon = 3 - d$. For the anomalous dimensions one finds

$$\eta_f = \epsilon/4,$$

$$\eta_b = \epsilon/2. \quad (31)$$

The fixed-point values for $\tilde{g}^2$, $\tilde{u}$, and $\tilde{\delta}$ are all of order ϵ. Terms neglected in our truncation are therefore of higher

order in ϵ. Note that the above results for η_f and η_b differ from the anomalous dimensions obtained for the Gross-Neveu model[27–29] already to leading order in ϵ.

At the quantum critical point, the fermionic properties of the system cannot be described in terms of Fermi-liquid theory. A finite fermion anomalous dimension entails a fermion propagator scaling with an anomalous power law as

$$G_{f\alpha}(\lambda\mathbf{k},\lambda\omega) \propto \lambda^{\eta_f-1} \quad (32)$$

for $\lambda \to 0$, corresponding to a nonanalytic frequency and momentum dependence of the self-energy. In particular,

$$\Sigma_{f\alpha}(\mathbf{0},\omega) \sim \omega^{1-\eta_f} \quad (33)$$

at the Fermi point $\mathbf{k}=\mathbf{0}$. In two dimensions we obtain $1 - \eta_f = 0.80$. A breakdown of Fermi-liquid theory in quantum critical interacting Fermi systems is very common.[4] For example, at a quantum critical point associated with a d-wave Pomeranchuk instability in two dimensions, the fermionic self-energy scales as $\omega^{2/3}$.[30,31] The fermion propagator also develops a small anomalous dimension in QED$_3$ (Ref. [32]) and in the Gross-Neveu model.[18,27–29]

Concerning the collective properties of the system, a finite boson anomalous dimension leads to anomalous scaling of the order parameter propagator

$$G_b(\lambda\mathbf{q},\lambda\omega) \propto \lambda^{\eta_b-2} \quad (34)$$

for $\lambda \to 0$, where $2 - \eta_b = 1.41$ in two dimensions.

In a different context, at the antiferromagnetic QCP of the spin-fermion model in two dimensions, Abanov *et al.*[7,8,33] obtained an anomalous momentum scaling $\propto |\mathbf{q}|^{-1.75}$ for the spin susceptibility within a perturbative $1/N$ calculation, where N is the number of hot spots on the Fermi surface.

Anomalous scaling of Dirac-type fermions and order parameter fields has also been found previously for certain quantum phase transitions in d-wave superconductors, where a second order parameter forms on top of d-wave superconductivity.[6,11]

B. Quantum critical flows in two dimensions

We now establish a continuous link between the bare action and the low-energy behavior of the *effective* action at the QCP in two dimensions. To this end, we compute the renormalization-group flow as a function of Λ by solving the flow Eqs. (26)–(28) numerically. The initial conditions of our parameters are chosen to match the bare action in Eq. (3), regularized by an additional term $\int \phi_q^*(q_0^2+\mathbf{q}^2)\phi_q$ as discussed in Sec. IV A 2: $u=0$, $Z_b=Z_f=g=1$. The Fermi velocity and the ultraviolet cutoff are set to unity, $\Lambda_0=v_f=1$. To reach the quantum critical point, the initial value of δ is tuned such that $\delta \to 0$ at the end of the flow. The critical initial value for δ obtained in this way is $\delta_c=0.0616$. This is smaller than the mean-field value $\delta_c^{\mathrm{MFT}}=\frac{1}{2\pi}$ obtained in Sec. III for two distinct reasons. One is a simple offset in the initial condition for the flow since the regulator functions, Eq. (17), are not infinite for $\Lambda=\Lambda_0$. Running a "mean-field flow" with these regulators but discarding bosonic fluctuations would yield $\delta_c^{\mathrm{MFT*}}=\frac{1}{4\pi} \approx 0.0796$. The remaining reduction is due to fluctuations.
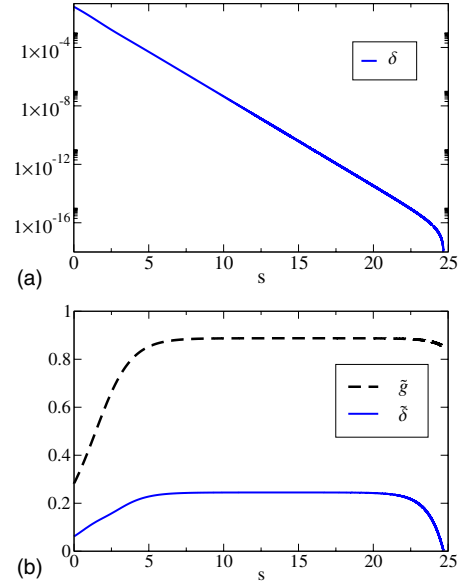

FIG. 6. (Color online) (a) Flow of the control parameter δ at the QCP. (b) Flows of the rescaled control parameter and fermion-boson vertex as a function of $s=-\ln[\Lambda/\Lambda_0]$. The ultraviolet (infrared) regime is on the left (right) side of the plots.

In Fig. 6(a), we show the flow of the control parameter at the QCP versus cutoff scale in a double logarithmic plot. We observe scaling behavior

$$\delta \sim \Lambda^{2-\eta_b} \quad (35)$$

over approximately 15 orders of magnitude (note the small values of δ on the vertical axis). Scaling stops at large s due to numerical errors. The power-law scaling of δ corresponds to the fixed-point plateaus of the *rescaled* control parameter $\tilde{\delta}$ in Fig. 6(b), where also the flow of the rescaled fermion-boson vertex is shown. The point we make here is that, starting from the microscopic model, the effective action is really attracted by the quantum critical fixed point.

In Fig. 7 we present flows for the fermionic and bosonic Z factors, Z_f and Z_b as well as the associated anomalous dimensions η_f and η_b. In Fig. 7(a), we observe that Z_b diverges as a power law: $Z_b \sim \Lambda^{-\eta_b}$, which corresponds to fixed-point plateaus of η_b shown in Fig. 7(b). The fermionic Z_f also diverges as a power law, $Z_f \sim \Lambda^{-\eta_f}$, with a smaller slope than Z_b, as reflected by the lower fixed-point plateau of η_f in Fig. 7(b). The numerical solution for the Z factors fulfils the relation, Eq. (30), and the fixed-point values match those of Fig. 5 at $d=2$.

We show flows of the ϕ^4 coupling in Fig. 8. Fermion fluctuations quickly generate u and then the interplay of fermionic and bosonic fluctuations leads to the power-law scaling behavior

$$u \sim \Lambda^{3-d-2\eta_b}, \quad (36)$$

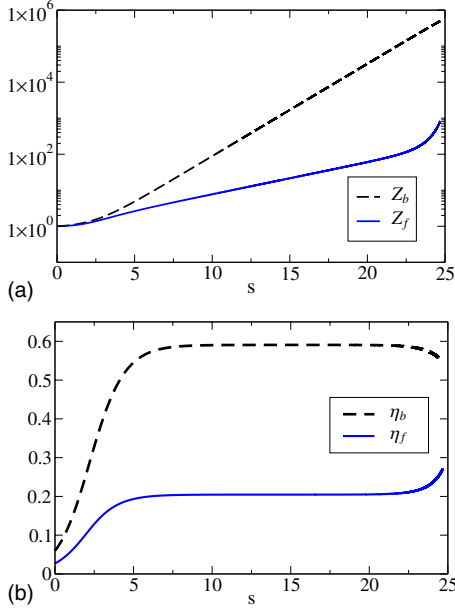accompanied by the fixed-point plateaus of $\tilde{u}$ in Fig. 8(b).

FIG. 7. (Color online) (a) Flows of the bosonic and fermionic frequency and momentum factors Z_b and Z_f. (b) Scaling plateaus of the fermion and boson anomalous dimensions at quantum criticality.

C. Quantum critical exponents

When approaching the quantum critical point along the control parameter axis, the susceptibility and the correlation length diverge as a power law,
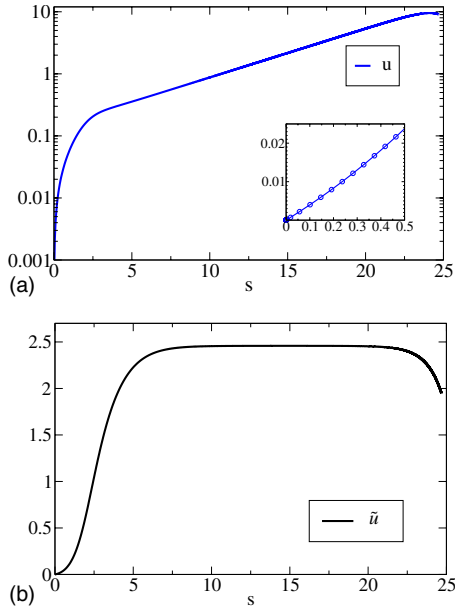
$$\chi \sim (\delta - \delta_c)^{-\gamma},$$

FIG. 8. (Color online) (a) Flow of the quartic coupling u. Inset: small-s behavior where fermionic fluctuations start generating u. (b) Fixed-point plateau of the rescaled ϕ^4 coupling.
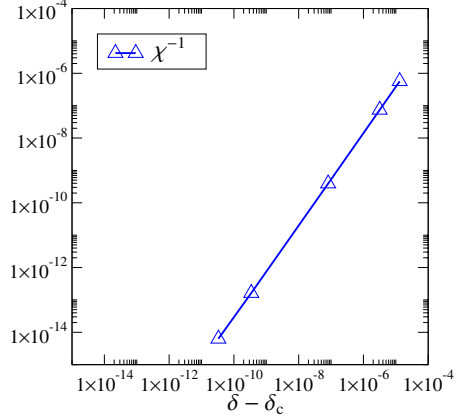

FIG. 9. (Color online) Logarithmic plot of the inverse susceptibility versus $\delta - \delta_c$ in $d=2$.

$$\xi \sim (\delta - \delta_c)^{-\nu}, \tag{37}$$

where δ is the bare bosonic mass ($=-1/U$). The inverse susceptibility is given by the renormalized bosonic mass at the end of the flow, $\chi^{-1} = \lim_{\Lambda \to 0} \delta$. Reading off the slope of a double-logarithmic plot of the susceptibility as a function of $\delta - \delta_c$, see Fig. 9, we find in two dimensions

$$\gamma = 1.4. \tag{38}$$

The correlation length exponent ν now follows from the general scaling relation $\gamma = \nu(2 - \eta_b)$.[34] With $\eta_b = 0.59$ in two dimensions, one obtains

$$\nu = 1.0. \tag{39}$$

VI. CONCLUSION

We have analyzed the quantum phase transition between a semimetal and a superfluid in a model of attractively interacting fermions with a Dirac cone dispersion. The model is a prototype for systems for which the Hertz-Millis approach to quantum phase transitions in itinerant Fermi systems is not applicable since integrating out the fermions leads to a singular Landau-Ginzburg functional. Using the functional RG framework, we have derived coupled flow equations for the gapless fermionic degrees of freedom and the bosonic order parameter fluctuations. Fermions and bosons acquire anomalous dimensions at the QCP in dimensions $d<3$. Consequently, both the fermion and the order parameter propagators are nonanalytic functions of frequency and momentum. In two dimensions, the fermionic self-energy scales as $\omega^{0.8}$ at low frequencies, implying the absence of fermionic quasiparticles and non-Fermi-liquid behavior. We have also computed the susceptibility and the correlation length exponents when approaching the QCP along the control parameter axis.

The strong impact of the gapless fermions on the order parameter interaction spoils the Hertz-Millis approach to quantum phase transitions, which is based on the Landau-Ginzburg paradigm. The fermionic anomalous dimension η_f influences critical exponents in a way that resembles the interplay of fermions and bosons in the Gross-Neveu

model.[18,29] Recently, the Gross-Neveu model has been proposed as an effective-field theory describing the quantum phase transition between a semimetal and an antiferromagnetic insulator for *repulsively* interacting electrons on the two-dimensional honeycomb lattice.[35]

In the present work we have focused on ground-state properties but an extension to finite temperatures should be straightforward. In particular, the quantum critical regime above the QCP in the (δ, T) plane could be studied with the same truncation of the functional RG hierarchy. Another interesting extension would be the inclusion of the pseudospin structure necessary to describe Dirac fermions on the honeycomb lattice. Our work may also serve as a guideline for the study of more complex quantum phase transitions in itinerant systems, for which the Hertz-Millis approach is not applicable, or at least questionable, such as certain magnetic transitions in low dimensions.

*p.strack@fkf.mpg.de

[1] J. A. Hertz, Phys. Rev. B **14**, 1165 (1976).

[2] A. J. Millis, Phys. Rev. B **48**, 7183 (1993).

[3] D. Belitz, T. R. Kirkpatrick, and T. Vojta, Rev. Mod. Phys. **77**, 579 (2005).

[4] H. v. Löhneysen, A. Rosch, M. Vojta, and P. Wölfle, Rev. Mod. Phys. **79**, 1015 (2007).

[5] B. L. Altshuler, L. B. Ioffe, and A. J. Millis, Phys. Rev. B **50**, 14048 (1994); **52**, 5563 (1995).

[6] M. Vojta, Y. Zhang, and S. Sachdev, Phys. Rev. Lett. **85**, 4940 (2000); Int. J. Mod. Phys. B **14**, 3719 (2000).

[7] A. Abanov and A. V. Chubukov, Phys. Rev. Lett. **84**, 5608 (2000).

[8] A. Abanov, A. V. Chubukov, and J. Schmalian, Adv. Phys. **52**, 119 (2003).

[9] J. Rech, C. Pepin, and A. V. Chubukov, Phys. Rev. B **74**, 195126 (2006).

[10] R. K. Kaul and S. Sachdev, Phys. Rev. B **77**, 155105 (2008).

[11] Y. Huh and S. Sachdev, Phys. Rev. B **78**, 064512 (2008).

[12] For an overview on the functional RG and references, see J. Berges, N. Tetradis, and C. Wetterich, Phys. Rep. **363**, 223 (2002).

[13] T. Baier, E. Bick, and C. Wetterich, Phys. Rev. B **70**, 125111 (2004).

[14] F. Schütz, L. Bartosch, and P. Kopietz, Phys. Rev. B **72**, 035107 (2005).

[15] P. Strack, R. Gersch, and W. Metzner, Phys. Rev. B **78**, 014522 (2008).

[16] H. Gies and J. Jaeckel, Phys. Rev. Lett. **93**, 110405 (2004).

[17] J. M. Pawlowski, D. F. Litim, S. Nedelko, and L. von Smekal, Phys. Rev. Lett. **93**, 152002 (2004).

[18] L. Rosa, P. Vitale, and C. Wetterich, Phys. Rev. Lett. **86**, 958 (2001); F. Höfling, C. Nowak, and C. Wetterich, Phys. Rev. B **66**, 205111 (2002).

[19] A. H. Castro Neto, F. Guinea, N. M. R. Peres, K. S. Novoselov, and A. K. Geim, Rev. Mod. Phys. **81**, 109 (2009).

[20] D. Gross and A. Neveu, Phys. Rev. D **10**, 3235 (1974).

[21] V. N. Popov, *Functional Integrals and Collective Excitations* (Cambridge University Press, Cambridge, 1987).

[22] E. Zhao and A. Paramekanti, Phys. Rev. Lett. **97**, 230404 (2006).

[23] B. Uchoa and A. H. Castro Neto, Phys. Rev. Lett. **98**, 146801 (2007).

[24] A. Neumayr and W. Metzner, Phys. Rev. B **58**, 15449 (1998).

[25] C. Kopper and J. Magnen, Ann. Henri Poincare **2**, 513 (2001).

[26] D. F. Litim, Phys. Rev. D **64**, 105007 (2001).

[27] A. N. Vasil'ev, S. E. Derkachev, N. A. Kivel', and A. S. Stepanenko, Theor. Math. Phys. **94**, 127 (1994); J. A. Gracey, Int. J. Mod. Phys. A **9**, 727 (1994).

[28] L. Kärkkäinen, L. Lacaze, P. Lacock, and B. Petersson, Nucl. Phys. **B415**, 781 (1994); **B438**, 650(E) (1995).

[29] J. Zinn-Justin, *Quantum Field Theory and Critical Phenomena* (Clarendon, Oxford, 1996).

[30] W. Metzner, D. Rohe, and S. Andergassen, Phys. Rev. Lett. **91**, 066402 (2003).

[31] L. Dell'Anna and W. Metzner, Phys. Rev. B **73**, 045127 (2006).

[32] M. Franz, Z. Tesanovic, and O. Vafek, Phys. Rev. B **66**, 054535 (2002).

[33] A. Abanov and A. V. Chubukov, Phys. Rev. Lett. **93**, 255702 (2004).

[34] N. Goldenfeld, *Lectures on Phase Transitions and the Renormalization Group* (Perseus, Oxford, 1992).

[35] I. F. Herbut, Phys. Rev. Lett. **97**, 146401 (2006); I. F. Herbut, V. Juričić, and O. Vafek, Phys. Rev. B **80**, 075432 (2009).